Cytokinin-Dependent Photorespiration and the Protection of Photosynthesis during Water Deficit[1][W][OA]

Rosa M. Rivero, Vladimir Shulaev, and Eduardo Blumwald*

Department Plant Sciences, University of California, Davis, California 95616 (R.M.R., E.B.); and Virginia Polytechnical Institute and State University, Virginia Bioinformatics Institute, Blacksburg, Virginia 24061 (V.S.)

We investigated the effects of P_{SARK}::*IPT* (for Senescence-Associated Receptor Kinase::Isopentenyltransferase) expression and cytokinin production on several aspects of photosynthesis in transgenic tobacco (*Nicotiana tabacum* cv SR1) plants grown under optimal or restricted (30% of optimal) watering regimes. There were no significant differences in stomatal conductance between leaves from wild-type and transgenic P_{SARK}-*IPT* plants grown under optimal or restricted watering. On the other hand, there was a significant reduction in the maximum rate of electron transport as well as the use of triose-phosphates only in wild-type plants during growth under restricted watering, indicating a biochemical control of photosynthesis during growth under water deficit. During water deficit conditions, the transgenic plants displayed an increase in catalase inside peroxisomes, maintained a physical association among chloroplasts, peroxisomes, and mitochondria, and increased the CO_2 compensation point, indicating the cytokinin-mediated occurrence of photorespiration in the transgenic plants. The contribution of photorespiration to the tolerance of transgenic plants to water deficit was also supported by the increase in transcripts coding for enzymes involved in the conversion of glycolate to ribulose-1,5-bisphosphate. Moreover, the increase in transcripts indicated a cytokinin-induced elevation in photorespiration, suggesting the contribution of photorespiration in the protection of photosynthetic processes and its beneficial role during water stress.

Cytokinins (CKs) are known to regulate several aspects of plant growth and development, including the response of plants to abiotic stress (Haberer and Kieber, 2002; Rivero et al., 2007). CKs regulate stomatal behavior (Reeves and Emery, 2007; Haisel et al., 2008; Hegele et al., 2008), the formation and protection of cellular structures (Chernyad'ev, 2005; Chiappetta et al., 2006), and the induction and activation of protein synthesis (Selivankina et al., 2004; Chernyad'ev, 2005). CKs maintain stomata open and thus increase stomatal conductance (g_s) and transpiration (E; Blackman and Davies, 1985; Jewer et al., 1985; Lechowski, 1997).

In general, there is a decrease in CK accumulation during drought stress, and the reduction in CKs can increase the shoot responses to increasing abscisic acid (ABA) concentrations during stress (Davies and Zhang, 1991), leading to stomatal closure and an increase in stomatal resistance (Goicoechea et al., 1997; Naqvi, 1999). These stress-induced changes in CKs and ABA promote early leaf senescence and hormonal changes leading to leaf abscission, contributing to a smaller canopy and reduced water loss. Although, under drought stress, this strategy can enhance the survival of perennial plants as well as promote the completion of the plant life cycle, it also reduces crop yield. Previous work showed that leaf senescence could be delayed in transgenic plants expressing isopentenyltransferase (IPT), an enzyme that catalyzes the rate-limiting step in CK synthesis (Pospíšilová et al., 2000), and also *ZOG1*, a gene coding for trans-zeatin *O*-glucosyltransferase (Haisel et al., 2008). Previously, a number of different strategies were used to drive *IPT* expression, among them its native promoter (Ondrej et al., 1989), a light-inducible promoter of a Rubisco subunit (Synkova et al., 1999), as well as heat shock-, copper-, and several senescence-inducible promoters (Beinsberger et al., 1991; Gan and Amasino, 1995; McKenzie et al., 1998; Pospíšilová et al., 2000, and refs. therein). Transgenic plants expressing *IPT* under the control of a constitutive or light-, copper-, or heat shock-inducible promoter lost their apical dominance, with poor suppression of auxiliary buds as well as poor root development. However, other transgenic plants expressing *IPT* under the control of senescence-activated promoters, such as *SAG12*, showed normal root development. Nevertheless, studies have shown that senescence-activated production of CKs caused an inhibition of chlorophyll breakdown in basal leaves of tobacco (*Nicotiana tabacum*) and alterations in source/sink relationships, namely a reduction in nitrogen mobilization to sinks (Jordi et al., 2000). Furthermore, it was also shown that senescence-activated production of

[1] This work was supported by the University of California Discovery Program, Arcadia Biosciences, and the Will W. Lester Endowment, University of California, Davis.

* Corresponding author; e-mail eblumwald@ucdavis.edu.

The author responsible for distribution of materials integral to the findings presented in this article in accordance with the policy described in the Instructions for Authors (www.plantphysiol.org) is: Eduardo Blumwald (eblumwald@ucdavis.edu).

[W] The online version of this article contains Web-only data.

[OA] Open Access articles can be viewed online without a subscription.

www.plantphysiol.org/cgi/doi/10.1104/pp.109.139378

CK markedly delayed flowering in lettuce (*Lactuca sativa*; McCabe et al., 2001).

In an effort to overcome adverse physiological effects resulting from the manipulation of CKs, we developed transgenic plants that expressed *IPT* under the control of *Senescence-Associated Receptor Kinase* (*SARK*; Hajouj et al., 2000), a maturation- and stress-inducible promoter (Rivero et al., 2007). Our results showed that the *IPT* gene was expressed not only during plant maturation but also at the onset of stress. The inducible characteristics of *SARK* allowed the production of CKs in all tissues facing drought-induced stress, which in turn enabled plants to mount a vigorous acclimation response resulting in enhanced drought tolerance with minimal yield loss (Rivero et al., 2007).

We have shown previously that following a severe drought treatment, the production of CKs in transgenic plants expressing P_{SARK}::*IPT* led to enhanced photosynthetic rates and water use efficiency (WUE). Moreover, the transgenic plants displayed minimal yield losses when watered with only a fraction of optimal water requirement (Rivero et al., 2007). Here, we investigated further the effects of P_{SARK}::*IPT* expression and CK production on several aspects of photosynthesis in transgenic tobacco plants grown under optimal or restricted watering regimes. Our results show that during water stress, the production of CKs resulted in the protection of biochemical processes associated with photosynthesis and in the induction of photorespiration during water stress, which may contribute to the protection of photosynthesis during water stress.

RESULTS

Effects of IPT Expression on Photosynthesis and WUE

To gain additional insight into the effects of endogenous CK production in plants expressing P_{SARK}::*IPT*, we measured and compared carbon assimilation (A), g_s, E, and WUE in wild-type plants and two independent lines of transgenic P_{SARK}::*IPT* plants grown under optimal and reduced watering regimes. We have shown previously that when wild-type plants and the two transgenic lines were grown under an optimal watering rate of 1,000 mL d^{-1} and a reduced watering rate of 300 mL d^{-1}, the biomass and seed yield of the wild-type plants was severely affected by the restricted water treatment, with reductions of 57% and 60%, respectively. However, the transgenic plants displayed minimal reduction (8%–14%) in biomass and seed yield (Rivero et al., 2007). Under the optimal watering regime, wild-type and P_{SARK}::*IPT* plants did not differ significantly in g_s and E (Fig. 1, A and B). P_{SARK}::*IPT* plants showed a reduction in E when grown at limited watering conditions, and E was further reduced in the wild-type plants (Fig. 1B). Under optimal watering regimes, wild-type and transgenic plants displayed similar photosynthetic rates (A), which declined slightly over the course of the experiment. A more pronounced reduction in A was seen under limited watering conditions (Fig. 1C). In both P_{SARK}::*IPT* lines, A was reduced by 25% and 50% after 40 and 75 d of growth, respectively. In contrast, wild-type plants showed 80% reduction in A after only 40 d of growth under water-limited conditions and total inhibition after 50 d (Fig. 1C). The reduction of A in wild-type plants grown under water-limiting conditions was paralleled by a severe reduction in WUE (Fig. 1D).

Biochemical Limitations to Photosynthesis by CKs

A reduction in A without a parallel reduction in g_s in wild-type plants grown under water-limiting conditions might suggest the occurrence of biochemical limitations restricting photosynthesis. In order to as-

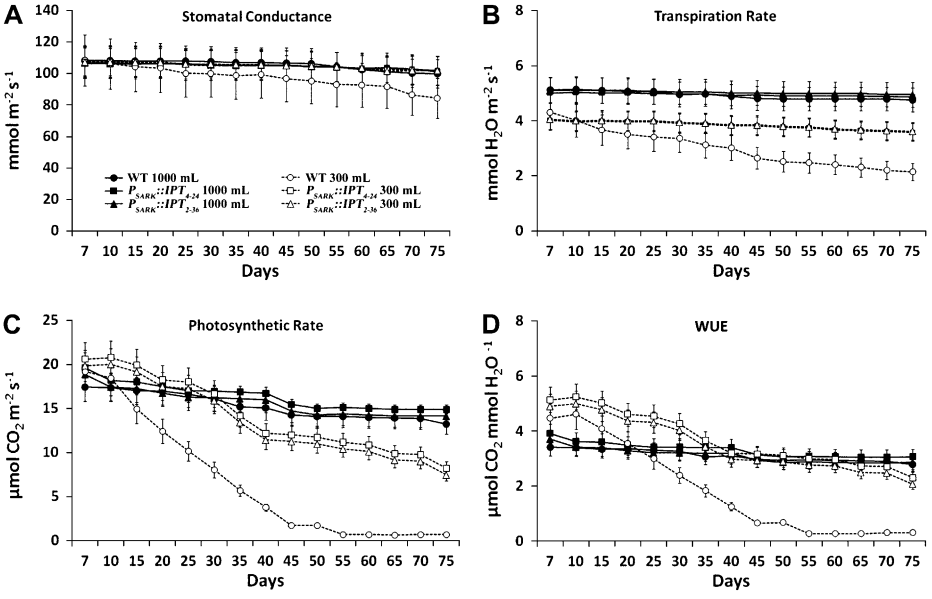

Figure 1. Comparison of photosynthetic parameters in wild-type plants (WT) and two transgenic lines expressing P_{SARK}::*IPT* measured over 75 d of growth under optimal conditions (1,000 mL d^{-1}; black symbols) or reduced watering conditions (300 mL d^{-1}; white symbols). The eighth fully expanded leaf was used for measurements using a LI-6400 gas-exchange system with a fixed chamber CO_2 concentration and light and temperature as described in "Materials and Methods." Values are means ± SE (n = 15).

sess the extent of the relative contribution of stomatal versus biochemical limitations to photosynthesis, we measured rates of CO_2 assimilation under varying intercellular CO_2 concentrations (Ci) and produced A/Ci curves. From the curves, one can calculate biochemical factors such as the maximum carboxylation rate of Rubisco (Vcmax), the maximum rate of the electron transport (Jmax) that is equivalent to the ribulose-1,5-bisP (RuBP) regeneration rate, as well as the use of triose-P (TPU; Farquhar et al., 1980; von Caemmerer, 2000). Under optimal watering conditions, wild-type and P_{SARK}::*IPT* transgenic plants showed similar A, which increased proportionally to the Ci until saturation was reached (Fig. 2A). Following 30 d of growth under restricted watering (300 mL d^{-1}), wild-type plants had significantly reduced A, while in both lines of P_{SARK}::*IPT* plants it remained similar to that of wild-type plants grown under optimal watering conditions (1,000 mL d^{-1}; Fig. 2B). A continued to diminish in wild-type plants grown under restricted watering after 40, 50, 60, and 70 d, while the assimilation rates of transgenic plants remained unaffected after 50 d and decreased to some extent afterward (Fig. 2, C–F). Under our experimental conditions, no significant differences were observed between the Vcmax of Rubisco in wild-type and transgenic plants grown under either limiting or optimal watering (Fig. 3A), suggesting that the reduction in photosynthesis observed in the wild-type plants grown under limiting water was not related to differ-

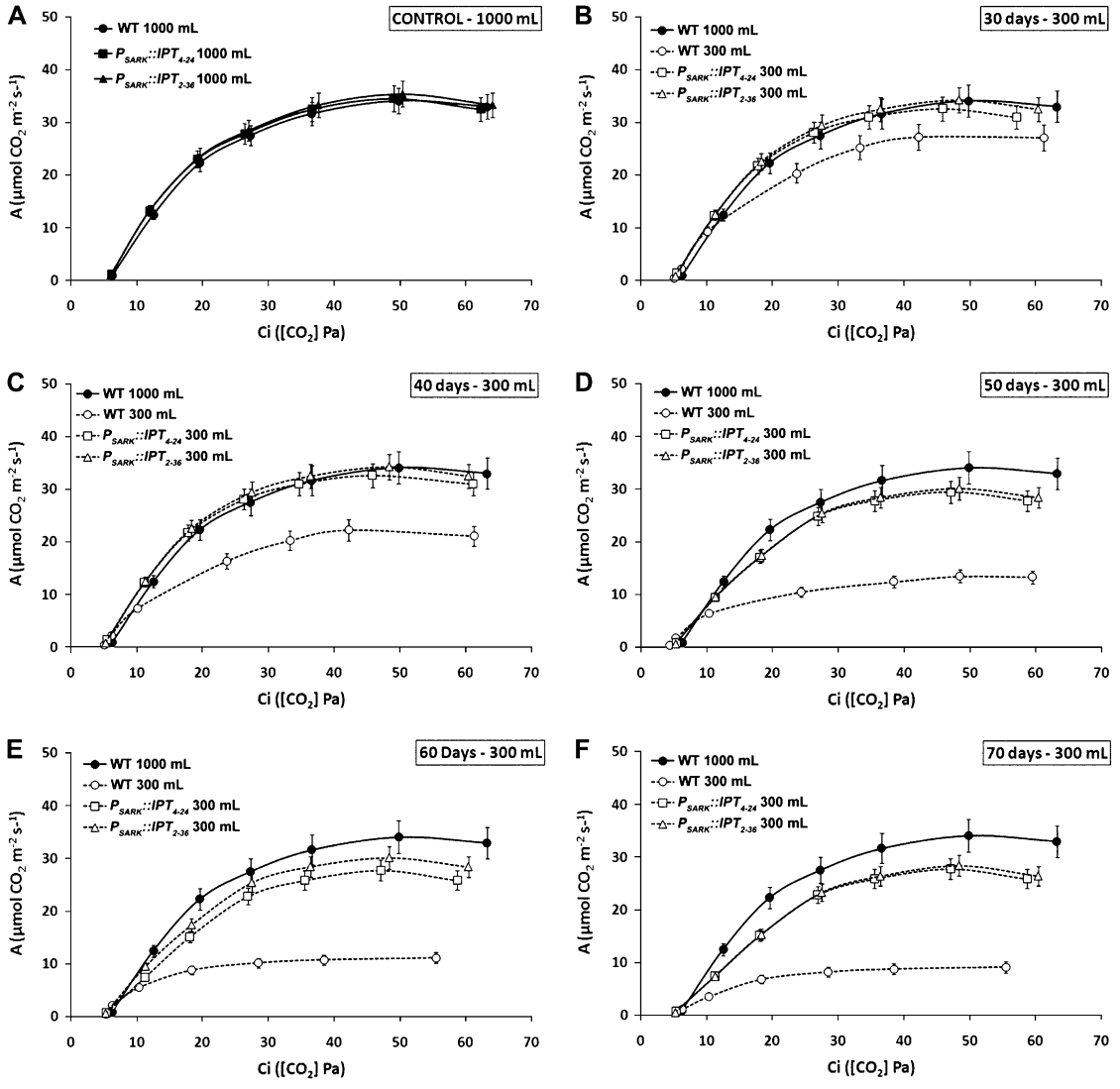

Figure 2. CO_2 assimilation rates at different intercellular CO_2 concentrations (A/Ci curves) of wild-type plants (WT) and two transgenic lines expressing P_{SARK}::*IPT* grown under optimal conditions (1,000 mL d^{-1}; A) or reduced watering conditions (300 mL d^{-1}; B–F) over 70 d. Wild-type plants growing under optimal watering were the control for every measurement. The eighth fully expanded leaf was used for measurements using a LI-6400 gas-exchange system with a fixed chamber CO_2 concentration and light and temperature as described in "Materials and Methods." Values are means ± SE (n = 15).

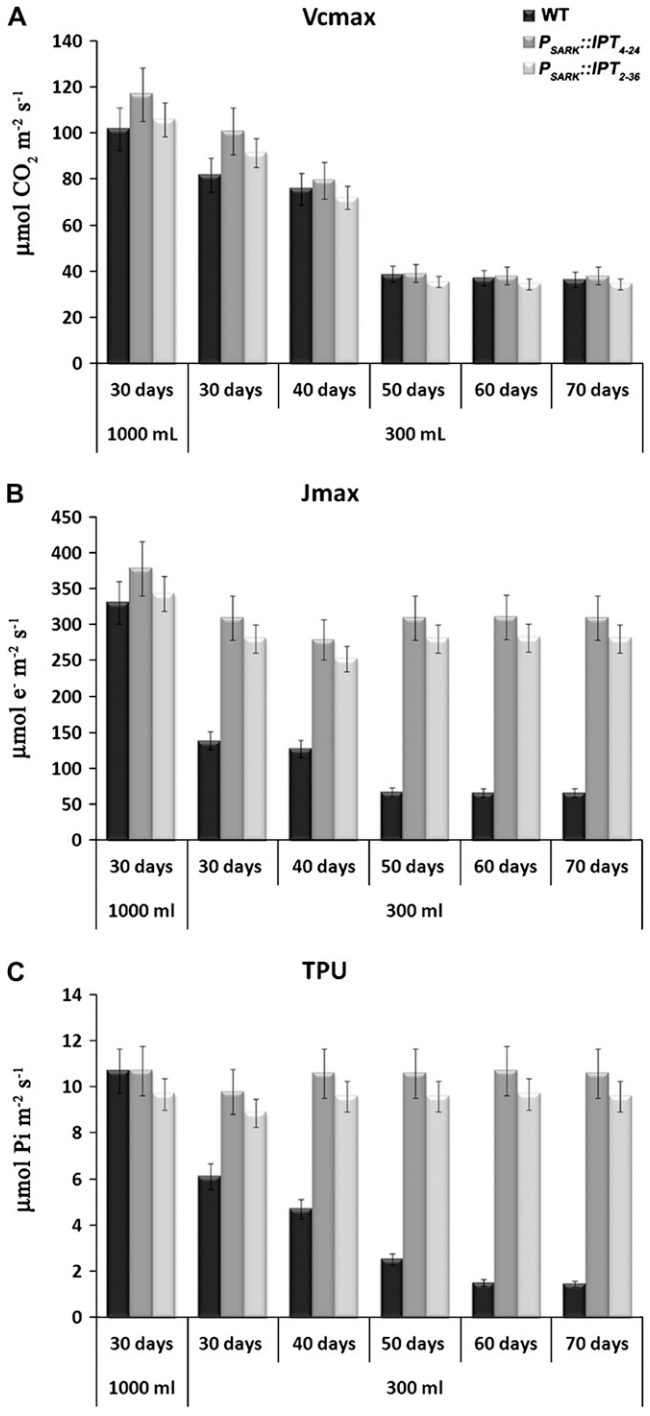

Figure 3. Vcmax (A), Jmax (B), and TPU (C) in wild-type plants (WT) and two transgenic lines expressing P_{SARK}::*IPT* grown under optimal conditions (1,000 mL d^{-1}) or reduced watering conditions (300 mL d^{-1}). The eighth fully expanded leaf was used for measurements using a LI-6400 gas-exchange system with a fixed chamber CO_2 concentration and light and temperature as described in "Materials and Methods." Values are means ± SE (n = 15).

ences in Rubisco activity. Although Jmax and TPU in transgenic plants expressing P_{SARK}::*IPT* were similar to those of wild-type plants grown under optimal watering conditions, wild-type plants displayed significant reductions in both Jmax and TPU after 30 d of growth under water deficit and were further reduced during extended growth periods with limited watering, thus suggesting a role of CKs in the protection of the electron transport, leading to the regeneration of RuBP and the capacity of the chloroplast reactions to use triose-Ps.

CK-Dependent Photorespiration

A morphological comparison between parenchyma cells from wild-type and P_{SARK}::*IPT* plants grown under optimal watering revealed interesting ultrastructural differences (Fig. 4). Distinct and large starch grains were seen in the chloroplasts of the transgenic plants (Fig. 4, B and D), which were sometimes also seen (albeit smaller) under limited water as well. Starch grains were not found in wild-type plants grown under either watering regime (Fig. 4, A and C). Wild-type plants also displayed unstacked thylakoids when grown under restricted watering (Fig. 4C), which is a typical response of chloroplasts to water stress (Sestak and Pospisilova, 1986; Zellnig et al., 2002). Notably, the parenchyma cells of P_{SARK}::*IPT* transgenic plants displayed an intracellular arrangement where chloroplasts, mitochondria, and peroxisomes were consis-

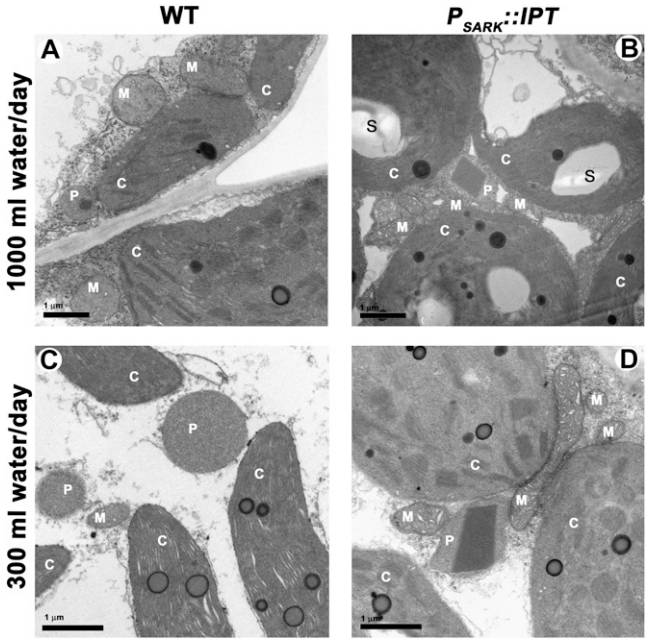

Figure 4. Electron micrographs of chloroplasts and surrounding organelles from wild-type plants (WT; A and C) and transgenic plants expressing P_{SARK}::*IPT* (B and D) grown under optimal conditions (1,000 mL d^{-1}; A and B) or reduced watering conditions (300 mL d^{-1}; C and D). C, Chloroplast; M, mitochondria; P, peroxisome; S, starch. Micrographs are from the eighth fully expanded leaf of 40- to 45-d-old plants. The crystalloids visible inside peroxisomes in transgenic plants are catalase. The micrographs are representative of four independent experiments (n = 4). Bars = 1 µm.

tently found in close proximity in all tissues examined (Fig. 4, B and D). This arrangement might indicate the occurrence of photorespiration in the transgenic plants (Ogren, 1984). In addition, large catalase crystals were seen in peroxisomes of transgenic plants grown under both optimal and restricted water regimes (Fig. 4, B and D). The presence of large catalase crystals correlates well with the reported increase in both catalase gene expression and catalase activity observed in P_{SARK}::*IPT* tobacco (Rivero et al., 2007).

Under restricted water conditions, wild-type and transgenic plants displayed similar Vcmax (Fig. 3A), suggesting possible differences in the oxygenase activity of Rubisco. We compared the CO_2 compensation point (Γ) of wild-type and transgenic plants (Fig. 5) because it has been shown previously that senescence or water stress can increase Γ with a concomitant increase in photorespiration (Smith et al., 1976). No significant differences were observed between wild-type and transgenic plants grown under optimal watering conditions, but differences were seen after 40 d of growth under water-limiting conditions (Fig. 5). While Γ decreased in wild-type plants, it increased progressively with time in transgenic plants (Fig. 5), suggesting the induction of photorespiration in P_{SARK}::*IPT* plants. Overall, our results suggest a relationship between the production of CKs (mediated by P_{SARK}::*IPT*) and the induction of photorespiration.

The abundance of transcripts coding for Rubisco (EC 4.1.1.39), phosphoglycolate phosphatase (PGPase; EC 3.1.3.18), glycolate oxidase (GO; EC 1.1.3.15), Gly decarboxylase (GDC; EC 2.1.2.10), Ser hydroxymethyltransferase (SHMT; EC 2.1.2.1), and glycerate kinase (GK; EC 2.7.1.31), key enzymes regulating photorespiration, was measured by quantitative PCR (Fig. 6, A and B). We normalized transcript comparisons to that of wild-type plants grown under control conditions and compared the transcripts of wild-type plants grown at reduced water with the transcripts of transgenic plants expressing P_{SARK}::*IPT* at both watering regimes (Fig. 6B). A quantitative comparison of the relative gene expression (qPCR) in wild-type plants indicated that water limitation caused a reduction in the expression of the selected transcripts except GK, where there were no significant differences with respect to its control ($\log_2 < 1.5$). However, the levels of these transcripts increased in P_{SARK}::*IPT* plants grown with optimal water and increased by 4-fold in plants grown under reduced watering (300 mL d^{-1}). Because photorespiration can generate metabolites such as Gly and Ser among other compounds that can be important for other cellular pathways (e.g. glutathione, amino acids, plant growth regulators, protein synthesis, etc.), we measured Gly, Ser, and glycerate (Fig. 6, C–E). Gly (Fig. 6C) and Ser (Fig. 6D) concentrations were higher in transgenic plants than in wild-type plants growing under control conditions. However, when compared with plants grown under restricted water, glycerate (Fig. 6E) was significantly higher in P_{SARK}::*IPT* tobacco. In order to assess metabolite flow during photorespiration, transcript levels of GDC and SHMT, key enzymes responsible for Gly degradation, were correlated to Gly concentrations. In wild-type plants, GDC and SHMT transcripts were negatively correlated with Gly concentration, supporting the accumulation of Gly in plants grown under reduced watering (Gly-GDC, $r = -0.991$***; Gly-SHMT, $r = -0.882$***). On the other hand, this correlation was positive in transgenic plants (Gly-GDC, $r = 0.802$**; Gly-SHMT, $r = 0.913$***), indicating flow through Ser formation. Although Ser concentrations were similar in both wild-type and transgenic plants expressing P_{SARK}::*IPT*, there was an increase in glycerate concentrations in transgenic plants grown under restricted water. The increase in glycerate concentrations together with the increase in GK transcripts would suggest an increased formation of glycerate to 3-phosphoglycerate that could be used for the regeneration of RuBP in the Calvin-Benson cycle.

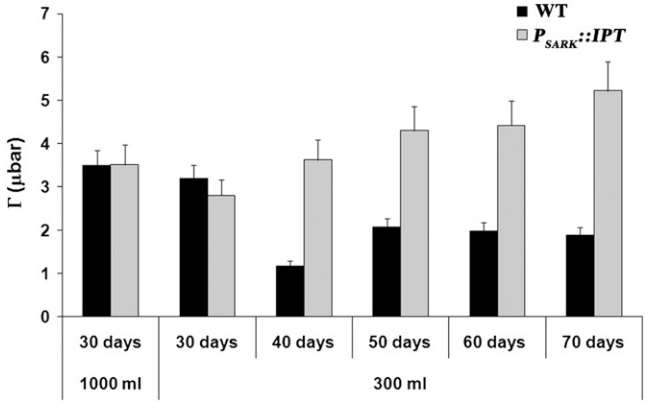

Figure 5. The Γ of wild-type plants (WT) and transgenic P_{SARK}::*IPT* plants grown for 70 d under optimal conditions (1,000 mL d^{-1}) or reduced watering conditions (300 mL d^{-1}). The eighth fully expanded leaf was used for measurements using a LI-6400 gas-exchange system with a fixed chamber CO_2 concentration and light and temperature as described in "Materials and Methods." Values are means ± SE ($n = 15$).

DISCUSSION

Stomata play a paramount role in the control of water loss and gas exchange in leaves. Most studies have shown that the increase in stomatal resistance during water deficit is the main factor limiting photosynthetic A (Chernyad'ev, 1997). During the onset of drought, stomatal conductivity declines before photosynthesis, and the inhibition of photosynthesis during mild stress is mainly due to the reduction of CO_2 diffusion (Cornic, 2000). Photosynthesis is not only restricted by stomatal limitations but also by nonstomatal limitations that impair metabolic reactions such as RuBP synthesis, ATP synthesis, and electron transfer, among others (Lawlor, 2002). In our experiments, leaf g_s of wild-type and transgenic plants

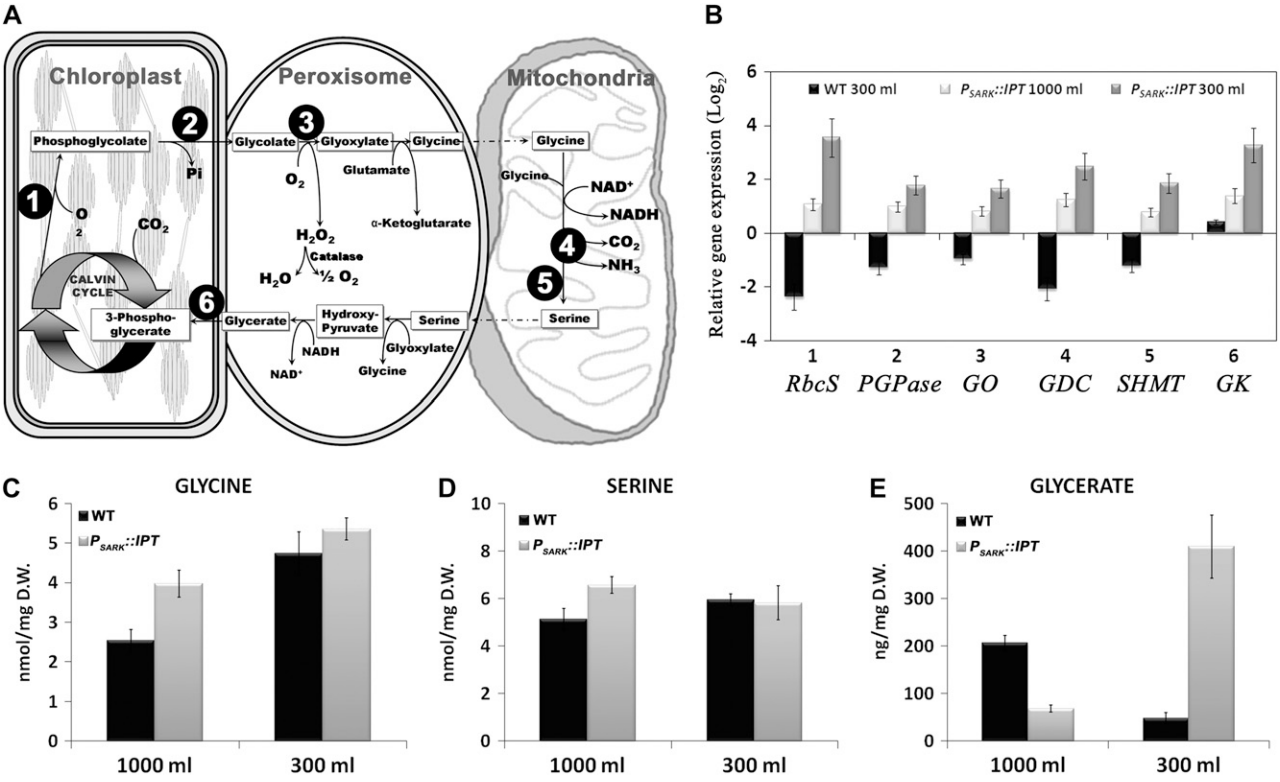

Figure 6. Photorespiration in wild-type plants (WT) and transgenic plants expressing P_{SARK}::*IPT* grown under optimal conditions (1,000 mL d^{-1}) or reduced watering conditions (300 mL d^{-1}). A, A schematic representation of the respiratory pathway of C_3 plants. 1, RbcS; 2, PGPase; 3, GO; 4, GDC; 5 SHMT; 6, GK. B, Relative expression of selected transcripts associated with photorespiration (1–6 as shown in A). C to E, Concentrations of selected photorespiratory metabolites. Analyses were performed in the eighth fully expanded leaf of individual plants. Values are means ± SE ($n = 6$). D.W., Dry weight.

expressing P_{SARK}::*IPT* was similar under optimal watering, but it was only slightly reduced in the wild-type plants grown under restricted watering (accompanied by a decrease in E). More pronounced was the decrease in A in wild-type plants after 20 d of growth under restricted watering. These results together with the biomass reduction observed in wild-type plants growing under restricted watering (Rivero et al., 2007) indicated that nonstomatal limitations to photosynthesis were the main factors inhibiting photosynthesis. Stomatal and nonstomatal limitations to photosynthesis were evaluated previously in four tobacco cultivars differing in drought tolerance (Vanrensburg and Kruger, 1993). In the drought-tolerant cultivars, high g_s was maintained in spite of higher rates of E, and the drought-induced decrease in A in the drought-sensitive cultivars was attributed to nonstomatal limitations (Vanrensburg and Kruger, 1993). The A/Ci response curves showed that while there was no difference in the maximum carboxylation rate of Rubisco of wild-type and transgenic plants, the regeneration of RuBP (Jmax) and TPU were significantly reduced in wild-type plants grown under restricted watering. Many studies have shown that a decrease in Jmax was correlated with a decrease in Rubisco activity (Hudson et al., 1992; Quick et al., 1992; Price et al., 1995). However, other studies have shown that RuBP regeneration can vary substantially without any changes in Rubisco activity (Vcmax; Ruuska et al., 1998; Harrison et al., 2001) and are in good agreement with our results.

CKs have been shown to stimulate stomatal opening (Dodd, 2003, and refs. therein), and CKs applied to isolated epidermis caused stomatal opening (Incoll and Whitelam, 1977). High concentrations of CKs can supersede the effects of ABA on stomata (Davies and Zhang, 1991), and many of the ABA-mediated processes induced by drought (closing of stomata, leaf abscission, etc.) are offset by CKs (Pospíšilová and Dodd, 2005). Moreover, the increase in endogenous CK content in transgenic plants expressing a bacterial *ipt* gene (Wang et al., 1997) or *zmp*, a gene coding a protein capable of cleaving CK glucosides, promoted increases in g_s and plant E in vivo (Pospíšilová et al., 1998). Plants transformed with P_{SARK}::*IPT* were shown to overexpress the *IPT* gene during maturity and during water shortage, and the enhanced expression of *IPT* was correlated with the increase of CKs in the leaves (Rivero et al., 2007).

The accumulation of ABA has also been correlated with drought tolerance (Thompson et al., 2007). A reciprocal relationship between ABA and CK contents during drought stress has been postulated (Pospíšilová

and Dodd, 2005), although the data supporting this notion are not conclusive (Yamaguchi-Shinozaki and Shinozaki, 2006). We have previously shown that under severe drought conditions, the increased drought tolerance displayed by the transgenic plants expressing P_{SARK}::*IPT* was not correlated with ABA accumulation (Rivero et al., 2007). Here, we examined the relative expression of some genes associated with ABA synthesis (*ABA3*, *NCED*, and *AAO2*) and degradation (*ABA 8-hydrolase*) in the wild-type and transgenic lines grown at optimal and restricted watering regimes (Supplemental Fig. S1). The expression of the genes involved in ABA synthesis was up-regulated in the wild-type plants grown under restricted water. In addition, the transcription of *ABA 8 hydrolase* was down-regulated. No significant differences in *ABA3*, *NCED*, and *ABA 8-hydrolase* transcripts were found in the transgenic lines, and *AAO2* was down-regulated in plants growing under restricted watering (Supplemental Fig. S1), supporting the lack of correlation between ABA levels and the enhanced tolerance to water deficit displayed by these plants (Rivero et al., 2007).

Our results showed that there were no significant differences in stomatal conductance between leaves from wild-type and P_{SARK}::*IPT* plants grown under optimal or restricted watering. On the other hand, there was a significant reduction in the Jmax and TPU only in wild-type plants during growth under restricted watering, indicating a biochemical control of photosynthesis during growth under water limitation. The increased IPT expression observed in both transgenic lines (Supplemental Fig. S2), the stress-induced increase in the CK content of transgenic plants expressing P_{SARK}::*IPT*, and the results presented in this work clearly support a role of endogenous CK production in the protection of biochemical processes associated with photosynthesis during water stress.

Plant adaptations to water deficiency are associated with functional and structural rearrangements of the photosynthetic machinery, and many of these changes are regulated by CKs and other phytohormones (Chernyad'ev, 2005). CKs accelerate the regeneration and the de novo formation of chloroplasts by regulating membrane formation and the synthesis of components of the electron transport system (Sestak and Pospisilova, 1986; Chernyad'ev, 2000; Pospíšilová et al., 2000; Veselova et al., 2006). The increase in catalase inside peroxisomes, the physical association between chloroplasts, peroxisomes, and mitochondria, and the increase in the CO_2 compensation point implied the occurrence of photorespiration in the transgenic plants. Photorespiration plays a key role in the protection of leaves against the presence of excessive reductant when CO_2 assimilation is restricted, facilitating energy dissipation and preventing photoinhibition (Osmond et al., 1997). Although under optimal conditions, photorespiration could be seen as an adverse process because of a reduction in photosynthesis and CO_2 assimilation during water stress (when CO_2 uptake and/or assimilation are diminished), photorespiration makes possible the supply of RuBP to the Calvin-Benson cycle (Wingler et al., 2000). In addition to its role in energy dissipation, photorespiration also generates metabolites that can be used by other biosynthetic pathways (Noctor et al., 2002). For example, photorespiration can generate Ser and Gly, which can be used for the synthesis of glutathione, a key component of the mechanism of protection against oxidative damage (Foyer and Noctor, 2000). The role of photorespiration during stress was assessed in heterologous barley (*Hordeum vulgare*) mutants with reduced activities in photorespiratory enzymes (Wingler et al., 1999). During drought, photosynthesis was lower in the mutants, indicating that photorespiration was increased during drought. The drought-induced increase in photorespiration was confirmed by the increase in Gly contents in drought-stressed leaves of the GDC mutant (Wingler et al., 1999). Rubisco is the main enzyme in the CO_2 assimilation pathway. This enzyme is constituted by two subunits, each one present in eight copies. The large subunits (55 kD) are encoded in the chloroplast, while the small subunits are encoded by a family of nuclear Rubisco small subunit (*RbcS*) genes. Mutants defective in *RbcS* genes displayed reduction in photosynthetic rates, suggesting that the Rubisco small subunit played an important role in the regulation of the carboxylase/oxygenase activity (Khrebtukova and Spreitzer, 1996). Also, photorespiration was suppressed in *rbcs* knockout mutants, suggesting a function of this subunit in the photorespiratory pathway (Dhingra et al., 2004). Our results showing a decrease in *RbcS* transcripts in wild-type plants growing under restricted water are in good agreement with the decrease in Rubisco carboxylase activity under these conditions (Fig. 3A). In contrast, the increase in *RbcS* transcripts in transgenic plants expressing P_{SARK}::*IPT* under both optimal and restricted water conditions suggests the CK-mediated transcriptional regulation of the gene.

The contribution of photorespiration to the tolerance of the transgenic plants to restricted watering regimes was also indicted by the increase in transcripts coding for enzymes involved in the conversion of glycolate to RuBP. Thus, transcripts coding for Rubisco, PGPase, GO, GDC, SHMT, and GK were increased in the transgenic plants expressing P_{SARK}::*IPT* but not in wild-type plants. Moreover, the increase in transcripts was enhanced in the transgenic plants grown under restricted watering conditions, suggesting a contribution of photorespiration in the protection of photosynthetic processes and a beneficial role during stress (Wingler et al., 2000), since transgenic plants displayed minimal yield loss under water-limiting conditions (Rivero et al., 2007).

Transgenic plants growing under control conditions displayed glycerate levels that were lower than those found in wild-type plants. However, GK transcription levels in the transgenic plants grown at optimal watering conditions were 4-fold higher than those in the wild type, suggesting the occurrence of photorespira-

tion and the flow and conversion of glycerate into 3-phosphoglycerate. This observation, together with the increases in GDC and SHMT, would indicate the flow of photorespiratory metabolites (Gly and Ser) to the regeneration of RuBP by the Calvin-Benson cycle. Because the capacity for RuBP regeneration (Jmax) was not affected in the transgenic plants grown at both restricted and optimal watering, a possible feedback on RuBP regeneration by the higher glycerate concentration in the transgenic plants under restricted water can be ruled out. Glycerate contents significantly increased in the transgenic plants growing under restricted watering. These results were unexpected, since under restricted watering the transcription levels of GK were more than 10-fold higher than those of wild-type plants growing under the same conditions. It is possible that the accumulation of glycerate under water deficit could lead to a feedback regulation of photosynthetic activity (Schimkat et al., 1990). In addition, it has been proposed that photorespiratory metabolites might also act as signals in the regulation of the expression of photorespiratory enzymes (Wingler et al., 2000). The increase in glycerate content in the transgenic plants grown under water deficit cannot be easily explained, and more research is needed to understand the role(s) of photorespiratory metabolites under water deficit.

In conclusion, here we have demonstrated a novel CK-mediated induction of photorespiration during water deficit. The induction of P_{SARK}::*IPT* expression and CK production in transgenic tobacco plants grown under restricted water resulted in the protection of a biochemical process associated with photosynthesis without significant effects on stomatal limitations. Our results indicate the possibility of generating transgenic plants with increased WUE and increased tolerance to water deficit.

MATERIALS AND METHODS

Experimental Design

Seeds of wild-type tobacco (*Nicotiana tabacum* 'SR1') and two independent transgenic lines expressing P_{SARK}::*IPT* were sown in soil (Metro-Mix 200; Sun Gro) in a growth chamber (500 μmol photons m^{-2} s^{-1}, 16-h photoperiod, 25°C) for 15 d until the appearance of the first two true leaves. During this time, no differences in germination time and in plant development between the wild type and both P_{SARK}::*IPT* lines were observed. Fifty plants of each genotype were transferred and transplanted (10-L pots) to a greenhouse, where they were grown for 1 week to allow acclimation of the plants to the new conditions (1,000 μmol photons m^{-2} s^{-1}, 16-h photoperiod, 28°C–30°C/23°C–25°C day/night). At this point, half of the wild-type plants and half of the P_{SARK}::*IPT* plants were selected to receive 1,000 mL of water per day (the amount of water necessary for tobacco plants to maintain cell turgor, designated as optimal watering conditions), whereas the other half of the plants received 300 mL of water per day (restricted watering conditions). This amount was considered to induce water deficit, because it produced a 50% yield reduction in the wild-type plants (Rivero et al., 2007). Plants were grown for 70 d, after which they started natural senescence. No water was allowed to drain from pots in any treatments.

CO_2-Exchange Measurements

Gas-exchange measurements were conducted in the eighth fully expanded leaf in each genotype (wild type, P_{SARK}::IPT_{4-24}, and P_{SARK}::IPT_{2-36}) with a gas-exchange system (LI-6400; Li-Cor). Leaves were first equilibrated at a photon density flux of 1,000 μmol m^{-2} s^{-1} for at least 20 min. After this, photosynthesis was induced with 1,000 μmol photons m^{-2} s^{-1} and 400 μmol mol^{-1} CO_2 surrounding the leaf (Ca). Leaf temperature was maintained at 25°C, and the leaf-to-air vapor pressure deficit was kept between 1 and 1.3 kPa. These conditions were kept constant for the determination of A, E, g_s, and WUE. WUE was calculated by the gas analyzer software as net photosynthesis per unit of water transpired, which is equal to the ratio between photosynthesis and transpiration rates (Dewar, 1997). The gas analyzer was calibrated daily and checked periodically. All measurements were repeated every 2 d and in four different experiments with the same greenhouse and gas analyzer conditions as described above and at four different seasons (spring, summer, autumn, and winter) in order to normalize the interference of weather conditions in our measurements.

CO_2 response curves were performed at steady state at least 30 min after clamping the leaf. Ten CO_2 response curves, corresponding to eighth fully expanded leaves of 15 different plants, were obtained per each plant genotype (the wild type and both P_{SARK}::*IPT* lines) and were repeated every 5 d. A and Ci were first measured at 400 μmol mol^{-1} Ca. Then, Ca was increased stepwise up to 1,800 μmol mol^{-1} and returned to its original value, followed by a stepwise decrease down to 0 μmol mol^{-1} Ca. A and Ci were measured at 12 different Ca values for each curve. From the A/Ci curves, the following photosynthetic parameters were calculated according to Long and Bernacchi (2003): Vcmax, Jmax, and TPU. In order to avoid miscalculation of A and Ci due to leakage into the gasket of the gas analyzer, we performed CO_2 response curves using an empty chamber. The values obtained for A and Ci in the empty chamber were compared with those of the chamber filled with a tobacco leaf and subtracted from the values obtained with the empty chamber.

The relation between A and Ci was fitted with the software Photosyn Assistant (Dundee Scientific). The program uses the model proposed by Farquhar et al. (1980), as subsequently modified by von Caemmerer and Farquhar (1981), Sharkey et al. (1985), Harley and Sharkey (1991), and Harley et al. (1992).

The Γ values were obtained from the initial slope of a CO_2 response curve at the lowest CO_2 concentration and could be obtained by fitting the equation and the A/Ci curve (Yang et al., 2008).

Electron Microscopy

For scanning electron microscopy, the eighth fully expanded leaves (leaf 8) of five different plants were fixed in an aqueous solution containing 2.5% glutaraldehyde and 4% paraformaldehyde in 0.05 M cacodylate buffer (pH 7.2) for 2 h. Samples were postfixed with 1% OsO_4 in the sample buffer during 1 h after the samples were dehydrated. Ultrathin sections (70 nm) of the parenchyma tobacco cells were obtained using a Reichert Ultracut ultramicrotome stained with uranyl acetate followed by lead citrate. The samples were observed with a Philips CM120 Biotwin lens (F.E.I.).

qPCR

cDNAs were obtained from two independent RNAs corresponding to the same sample using the SuperScript VILO synthesis kit (Invitrogen). This procedure was done with tissues from wild-type plants and both P_{SARK}::*IPT* plants growing under control conditions (1,000 mL d^{-1}) or under water deficit (300 mL d^{-1}) so that every sample was represented by two independent cDNAs.

From each cDNA, three replicates were placed on a 96-well plate, so that every sample was represented by six replicates. For all targets analyzed, the primers were designed using ABI Primer Express software. For *IPT* expression, the primers used were *IPT*-forward (5′-CCAAGGCCAGAGTTAAGCAG-3′) and *IPT*-reverse (5′-TTTGCGTCAAGCTGCAATAG-3′). For ABA metabolism, four different targets were analyzed: *ABA3*, *NCED*, and *AAO2* for ABA synthesis and *ABA 8-hydrolase* for ABA degradation. The primers used for the amplification of these products were *ABA3*-forward (5′-AGCACCAGGATTGCAAAAAC-3′) and *ABA3*-reverse (5′-CTTTTGGCACTGAAGCATGA-3′), *NECD*-forward (5′-TCGTCTTCTCCTTGCTGTT-3′) and *NCED*-reverse (5′-TAGAAGCCGGAATGGTGAAC-3′), *AAO2*-forward (5′-CGGCGACTCCATCTGTTAAT-3′) and *AAO2*-reverse (5′-GATGAAGAAGGTCGGAGCTG-3′), and *ABA 8-hydrolase*-forward (5′-CCTACCACTTCCCACCTGAA-3′) and *ABA 8-hydrolase*-reverse (5′-GGAAGGTGATGCCTTTGTTC-3′). From the photorespiratory pathway, six different targets were analyzed (Rubisco small subunit [*smRubisco*], *PGPase*, *GO*, *GDC*, *SHMT*, and *GK*). The primers were designed using the ABI Primer Express Software, and

their sequences are as follows: *smRubisco*-forward (5′-AGTGCGGCAACGGTAATATC-3′) and *smRubisco*-reverse (5′-TCAACAAAGTCCGGAGAACC-3′), *PGPase*-forward (5′-GGCTCTACAAAGCGTGAACC-3′) and *PGPase*-reverse (5′-GAGTTTTGCAGCCACCATTT-3′), *GO*-forward (5′-CTACTATGCCTCGGGAGCTG-3′) and *GO*-reverse (5′-CCTTCAGGATGTGCCATTTT-3′), *GDC*-forward (5′-CAACAGCCAACGCACTAAGA-3′) and *GDC*-reverse (5′-GCTCCAAAACTGCTTCCTTG-3′), *SHMT*-forward (5′-CAAAGCAACTGAATGCTCCA-3′) and *SMHT*-reverse (5′-TGACTGATCCAACTGCTTGC-3′), and *GK*-forward (5′-GCCTCAAGGATGTGGAAAAA-3′) and *GK*-reverse (5′-ATCATGGCTTCCAGCATTTC-3′). Two independent internal controls (*18S* rRNA and *Ubiquitin-Conjugated Protein2* [*UBQ2*]), whose expression did not change over the amplification in the different samples, were processed in parallel. The primers used were as follows: *18S*-forward (5′-ATGATAACTCGACGGATCGC-3′) and *18S*-reverse (5′-CTTGGATGTGGTAGCCGTTT-3′) and *UBQ2*-forward (5′-TGAGGATTACCCCAACAAGC-3′) and *UBQ2*-reverse (5′-AGGTGAGTTGGGGTTTGGAT-3′). The amplification was performed in a total reaction volume of 20 μL. Reactions included 2 μL of template, 10 μL of Fast SYBR Green Master Mix, 0.9 μL of reverse primer, 0.9 μL of forward primer, and sterile molecular biology-grade water to a total volume of 20 μL. All PCRs were performed with the exact reaction cycling conditions as follows: 95°C for 10 min followed by 40 cycles of 95°C for 3 s and 60°C for 30 s. A melt curve for every target analyzed was included with the following conditions: 95°C for 15 s, 60°C for 1 min, and 95°C for 15 s. Amplification and data analysis were carried out on an ABI StepOne Plus real-time PCR system (Applied Biosystems) taking as internal controls *18S* rRNA and *UBQ2* and as a sample control wild-type plants growing under control conditions (1,000 mL d^{-1}). All template and primer concentrations were optimized for the reactions.

Metabolite Analysis

Sample Extraction

Ten milligrams of freeze-dried leaf was ground using 3.2-mm chrome-steel beads in a Retsch mixer mill, followed by extraction with 500 μL of 50:50 methanol:water spiked with 2 μg L^{-1} of the internal standards. After the extraction buffer was added, the mixture was stirred on the Retsch mill for 1 min at 30 repetitions s^{-1}, sonicated for 1 min in an ultrasonic bath, and incubated on dry ice for 5 min. Three cycles of sonication and dry ice incubation were carried out before spinning out the extract for 15 min at 13,000 rpm. Clear supernatant was transferred into limited-volume HPLC vials and analyzed by liquid chromatography-mass spectrometry (LC-MS) and liquid chromatography-tandem mass spectrometry (LC-MS/MS).

Metabolite Quantitation

Glycerate was measured using hydrophilic interaction LC-MS/MS as described previously (Bajad et al., 2006). LC-MS/MS was performed on the LC-10ADvp chromatographic system (Shimadzu) coupled to a mass spectrometer. LC separation was performed on a Phenomenex 250- × 2-mm Luna 5-μm aminopropyl column using gradient elution with 20 mM ammonium acetate + 20 mM ammonium hydroxide in 95:5 water:acetonitrile, pH 9.45 (solvent A), and acetonitrile (solvent B). The gradient profile was as follows: time 0, 75% B; 15 min, 0% B; 38 min, 0% B; 40 min, 85% B; 50 min, 85% B. LC conditions were as follows: autosampler temperature, 4°C; column temperature, 15°C; injection volume, 20 μL; solvent flow rate, 250 μL min^{-1}. Mass spectrometry analysis was performed on a TSQ Quantum triple quadrupole mass spectrometer (Thermo Electron). Column effluent was introduced into the electrospray ionization (ESI) ion source using a fused silica capillary. The mass spectrometer was operated in single reaction monitoring mode. Mass spectrometer conditions were as follows: ESI spray voltage, 3,200 V in positive mode and 3,000 V in negative mode; nitrogen sheath gas, 30 psi; nitrogen auxiliary gas, 10 psi; argon collision gas, 1.5 mTorr; ion transfer capillary temperature, 325°C. Scan time was 0.1 s for each single reaction monitoring with a scan width of 1 nm/z. Quantitation was performed using calibration curves with stable isotope-labeled internal standard malic-2,3,3-d3 acid (C/D/N Isotopes) that was added to each sample. A commercially available pure form of DL-glyceric acid was purchased from MB Biomedicals and used to prepare calibration curves.

Amino acids were measured using the precolumn AccQ·Tag Ultra UPLC derivatization kit (Waters Corporation). Reagents for derivatization were prepared and derivatization was performed according to the manufacturer's protocol. For derivatization, 80 μL of borate buffer was added to 10 μL of the extract, followed by 20 μL of reagent solution. The reaction mixture was mixed immediately and heated to 55°C for 5 min.

LC-MS-photodiode array analysis was performed on an LC-MS system composed of the Waters Acquity UPLC system (Waters Corporation) equipped with the Acquity photodiode array detector interfaced with the ThermoFisher LTQ mass spectrometer (ThermoFisher). UPLC separation was performed on the AccQ·Tag Ultra column (1.7 μm, 100 mm × 2.1 mm i.d.) from Waters. The flow rate was 0.7 mL min^{-1}, and the column temperature was kept at 55°C. The injection volume was 2 μL, and the detection wavelength was set at 260 nm. The solvent system consisted of two eluents: AccQ·Tag Ultra eluent A concentrate (5%, v/v) and water (95%, v/v; eluent A) and AccQ·Tag Ultra eluent B. The profile was as follows: 0 to 0.54 min, 99.9% A and 0.1% B; 5.74 min, 90.9% A and 9.1% B; 7.74 min, 78.8% A and 21.2% B; 8.04 min, 40.4% A and 59.6% B; 8.73 to 10 min, 99.9% A and 0.1% B. Mass spectrometry detection was performed on the LTQ linear ion trap mass spectrometer (ThermoFisher). Column effluent was ionized by ESI, and the mass spectrometer was operated in full-scan positive mode under the following conditions: ESI spray voltage, 3,500 V; nitrogen sheath gas, 32 angstrom units; nitrogen auxiliary gas, 4 angstrom units; ion transfer capillary temperature, 275°C. Amino acid quantitation was performed using calibration curves with stable isotope-labeled internal standards L-Ser-2,3,3-d_3 (Cambridge Isotopes Laboratories) and L-Pro-2,5,5-d_3 (C/D/N Isotopes) that were added to each sample. Commercially available forms of the amino acids were purchased from Sigma-Aldrich and used to prepare the calibration curves.

Statistical Analysis

ANOVA was conducted using Student's *t* test in Statistica (version 6.0; StatSoft). For all parameters, either the Student's *t* test or the nonparametric Mann-Whitney *U* test for independent samples, in accordance with the preliminary Levene's test for equality of variances ($P < 0.05$), was used to test the differences between transgenic and wild-type plants and between control and restricted water amounts. A correlation analysis was also performed between the different variables. Levels of significance are represented by asterisks as follows: * $P < 0.05$, ** $P < 0.01$, *** $P < 0.001$; NS indicates not significant ($P > 0.05$).

Supplemental Data

The following materials are available in the online version of this article.

Supplemental Figure S1. Relative changes in the expression of genes involved in ABA synthesis (*ABA3*, *NCED*, and *AAO2*) and degradation (*ABA 8-hydrolase*).

Supplemental Figure S2. Relative expression of IPT by real-time PCR in two transgenic lines expressing P_{SARK}::*IPT*.

ACKNOWLEDGMENTS

We thank Dr. Elias Bassil and other members of the Blumwald laboratory for helpful discussions.

Received April 1, 2009; accepted April 25, 2009; published May 1, 2009.

LITERATURE CITED

Bajad SU, Lu WY, Kimball EH, Yuan J, Peterson C, Rabinowitz JD (2006) Separation and quantitation of water soluble cellular metabolites by hydrophilic interaction chromatography-tandem mass spectrometry. J Chromatogr A **1125:** 76–88

Beinsberger SEI, Valcke RLM, Deblaere RY, Clijsters HMM, Degreef JA, Vanonckelen HA (1991) Effects of the introduction of *Agrobacterium tumefaciens* T-DNA *ipt* gene in *Nicotiana tabacum* L. cv. Petit Havana SR1 plant cells. Plant Cell Physiol **32:** 489–496

Blackman PG, Davies WJ (1985) Root to shoot communication in maize plants of the effects of soil drying. J Exp Bot **36:** 39–48

Chernyad'ev II (1997) Plant photosynthesis under conditions of water stress and the protective effect of cytokinins: a review. Appl Biochem Microbiol **33:** 1–12

Chernyad'ev II (2000) Photosynthesis in sugar beet plants treated with benzyladenine and metribuzin during leaf ontogeny. Russ J Plant Physiol **47:** 161–167

Chernyad'ev II (2005) Effect of water stress on the photosynthetic apparatus of plants and the protective role of cytokinins: a review. Appl Biochem Microbiol **41:** 115–128

Chiappetta A, Michelotti V, Fambrini M, Bruno L, Salvini M, Petrarulo M, Azmi A, Van Onckelen H, Pugliesi C, Bitonti MB (2006) Zeatin accumulation and misexpression of a class I knox gene are intimately linked in the epiphyllous response of the interspecific hybrid EMB-2 (Helianthus annuus x Helianthus tuberosus). Planta **223:** 917–931

Cornic G (2000) Drought stress inhibits photosynthesis by decreasing stomatal aperture: not by affecting ATP synthesis. Trends Plant Sci **5:** 187–188

Davies WJ, Zhang JH (1991) Root signal and the regulation of growth and development of plants in drying soil. Annu Rev Plant Physiol Plant Mol Biol **42:** 55–76

Dewar RC (1997) A simple model of light and water use evaluated for *Pinus radiata*. Tree Physiol **17:** 259–265

Dhingra A, Portis AR, Daniell H (2004) Enhanced translation of a chloroplast-expressed RbcS gene restores small subunit levels and photosynthesis in nuclear RbcS antisense plants. Proc Natl Acad Sci USA **101:** 6315–6320

Dodd IC (2003) Hormonal interactions and stomatal responses. J Plant Growth Regul **22:** 32–46

Farquhar GD, Caemmerer SV, Berry JA (1980) A biochemical model of photosynthetic CO_2 assimilation in leaves of C-3 species. Planta **149:** 78–90

Foyer CH, Noctor G (2000) Oxygen processing in photosynthesis: regulation and signalling. New Phytol **146:** 359–388

Gan SS, Amasino RM (1995) Inhibition of leaf senescence by autoregulated production of cytokinin. Science **270:** 1986–1988

Goicoechea N, Antolin MC, Sánchez-Díaz M (1997) Gas exchange is related to the hormone balance in mycorrhizal or nitrogen-fixing alfalfa subjected to drought. Physiol Plant **100:** 989–997

Haberer G, Kieber JJ (2002) Cytokinins: new insights into a classic phytohormone. Plant Physiol **128:** 354–362

Haisel D, Vankova R, Synkova H, Pospisilova J (2008) The impact of transzeatin *O-glucosyltransferase* gene over-expression in tobacco on pigment content and gas exchange. Biol Plant **52:** 49–58

Hajouj T, Michelis R, Gepstein S (2000) Cloning and characterization of a receptor-like kinase gene associated with senescence. Plant Physiol **124:** 1305–1314

Harley PC, Loreto F, Dimarco G, Sharkey TD (1992) Theoretical considerations when estimating the mesophyll conductance to CO_2 flux by analysis of the response of photosynthesis to CO_2. Plant Physiol **98:** 1429–1436

Harley PC, Sharkey TD (1991) An improved model of C3 photosynthesis at high CO_2: reversed O_2 sensitivity explained by lack of glycerate reentry into the chloroplast. Photosynth Res **27:** 169–178

Harrison EP, Olcer H, Lloyd JC, Long SP, Raines CA (2001) Small decreases in SBPase cause a linear decline in the apparent RuBP regeneration rate, but do not affect Rubisco carboxylation capacity. J Exp Bot **52:** 1779–1784

Hegele M, Manochai P, Naphrom D, Sruamsiri P, Wunsche J (2008) Flowering in langan (*Dimocarpus longan* L.) induced by hormonal changes following $KClO_3$ applications. Eur J Hortic Sci **73:** 49–54

Hudson GS, Evans JR, Voncaemmerer S, Arvidsson YBC, Andrews TJ (1992) Reduction of ribulose-1,5-bisphosphate carboxylase oxygenase content by antisense RNA reduces photosynthesis in transgenic tobacco plants. Plant Physiol **98:** 294–302

Incoll LD, Whitelam GC (1977) Effect of kinetin on stomata of grass *Anthephora pubescens* Nees. Planta **137:** 243–245

Jewer PC, Neales TF, Incoll LD (1985) Stomatal responses to carbon dioxide of isolated epidermis from a C3 plant, the Argenteum mutant of *Pisum sativum* L., and a crassulacean-acid-metabolism plant *Kalanchoe daigremontiana* Hamet and Perr. Planta **164:** 495–500

Jordi W, Schapendonk A, Davelaar E, Stoopen GM, Pot CS, De Visser R, Van Rhijn JA, Gan S, Amasino RM (2000) Increased cytokinin levels in transgenic P-SAG12-IPT tobacco plants have large direct and indirect effects on leaf senescence, photosynthesis and N partitioning. Plant Cell Environ **23:** 279–289

Khrebtukova I, Spreitzer RJ (1996) Elimination of the Chlamydomonas gene family that encodes the small subunit of ribulose-1,5-bisphosphate carboxylase oxygenase. Proc Natl Acad Sci USA **93:** 13689–13693

Lawlor DW (2002) Limitation to photosynthesis in water-stressed leaves: stomata vs. metabolism and the role of ATP. Ann Bot (Lond) **89:** 871–885

Lechowski Z (1997) Stomatal response to exogenous cytokinin treatment of the hemiparasite *Melampyrum arvense* L before and after attachment to the host. Biol Plant **39:** 13–21

Long SP, Bernacchi CJ (2003) Gas exchange measurements, what can they tell us about the underlying limitations to photosynthesis? Procedures and sources of error. J Exp Bot **54:** 2393–2401

McCabe MS, Garratt LC, Schepers F, Jordi WJRM, Stoopen GM, Davelaar E, van Rhijn JHA, Power JB, Davey MR (2001) Effects of P-SAG12-IPT gene expression on development and senescence in transgenic lettuce. Plant Physiol **127:** 505–516

McKenzie MJ, Mett V, Reynolds PHS, Jameson PE (1998) Controlled cytokinin production in transgenic tobacco using a copper-inducible promoter. Plant Physiol **116:** 969–977

Naqvi S (1999) Plant hormones and stress phenomena. *In* M Pessarakli, ed, Handbook of Plant and Crop Physiology. Marcel Dekker, New York, pp 645–660

Noctor G, Veljovic-Jovanovic S, Driscoll S, Novitskaya L, Foyer CH (2002) Drought and oxidative load in the leaves of C-3 plants: a predominant role for photorespiration? Ann Bot (Lond) **89:** 841–850

Ogren WL (1984) Photorespiration: pathways, regulation, and modification. Annu Rev Plant Physiol Plant Mol Biol **35:** 415–442

Ondrej M, Eder J, Hrouda M, Machackova I, Vlasak J (1989) Free auxin level and inheritance of introduced markers in tobacco transformed by binary vector based on A4 Ri plasmid. Biol Plant **31:** 286–291

Osmond B, Badger M, Maxwell K, Bjorkman O, Leegood R (1997) Too many photos: photorespiration, photoinhibition and photooxidation. Trends Plant Sci **2:** 119–121

Pospíšilová J, Dodd IC (2005) Role of plant growth regulators in stomatal limitation to photosynthesis during water stress. *In* M Pessarakli, ed, Handbook of Photosynthesis, Ed 2, Revised and Expanded. Marcel Dekker, New York, pp 811–825

Pospíšilová J, Synkova H, Machackova I, Catsky J (1998) Photosynthesis in different types of transgenic tobacco plants with elevated cytokinin content. Biol Plant **40:** 81–89

Pospíšilová J, Synkova H, Rulcova J (2000) Cytokinins and water stress. Biol Plant **43:** 321–328

Price GD, Evans JR, von Caemmerer S, Yu JW, Badger MR (1995) Specific reduction of chloroplast glyceraldehyde-3-phosphate dehydrogenase activity by antisense RNA reduces CO_2 assimilation via a reduction in ribulose-bisphosphate regeneration in transgenic tobacco plants. Planta **195:** 369–378

Quick WP, Fichtner K, Schulze ED, Wendler R, Leegood RC, Mooney H, Rodermel SR, Bogorad L, Stitt M (1992) Decreased ribulose-1,5-bisphosphate carboxylase-oxygenase in transgenic tobacco transformed with antisense *rbcs* impact on photosynthesis in conditions of altered nitrogen supply. Planta **188:** 522–531

Reeves I, Emery RJN (2007) Seasonal patterns of cytokinins and microclimate and the mediation of gas exchange among canopy layers of mature *Acer saccharum* trees. Tree Physiol **27:** 1635–1645

Rivero RM, Kojima M, Gepstein A, Sakakibara H, Mittler R, Gepstein S, Blumwald E (2007) Delayed leaf senescence induces extreme drought tolerance in a flowering plant. Proc Natl Acad Sci USA **104:** 19631–19636

Ruuska S, Andrews TJ, Badger MR, Hudson GS, Laisk A, Price GD, von Caemmerer S (1998) The interplay between limiting processes in C-3 photosynthesis studied by rapid-response gas exchange using transgenic tobacco impaired in photosynthesis. Aust J Plant Physiol **25:** 859–870

Schimkat D, Heineke D, Heldt HW (1990) Regulation of sedoheptulose-1,7-bisphosphatase by sedoheptulose-7-phosphate and glycerate, and of fructose-1,6-bisphosphatase by glycerate in spinach chloroplasts. Planta **181:** 97–103

Selivankina SY, Karavaiko NN, Maslova GG, Zubkova NK, Prokoptseva OS, Smith AR, Hall MA, Kulaeva ON (2004) Cytokinin-binding protein from Arabidopsis thaliana leaves participating in transcription regulation. Plant Growth Regul **43:** 15–26

Sestak Z, Pospisilova J (1986) Water stress induced changes in photosynthetic characteristics of chloroplasts and their dependence on leaf development. Photobiochem Photobiophys **12:** 163–172

Sharkey TD, Berry JA, Raschke K (1985) Starch and sucrose synthesis in *Phaseolus vulgaris* as affected by light, CO_2, and abscisic acid. Plant Physiol **77:** 617–620

Smith EW, Tolbert NE, Ku HS (1976) Variables affecting CO_2 compensation point. Plant Physiol **58:** 143–146

Synkova H, Van Loven K, Pospisilova J, Valcke R (1999) Photosynthesis of transgenic *Pssu-ipt* tobacco. J Plant Physiol **155:** 173–182

Thompson AJ, Andrews J, Mulholland BJ, McKee JMT, Hilton HW, Black CR, Taylor IB (2007) Overproduction of abscisic acid in tomato increases transpiration efficiency and root hydraulic conductivity and influences leaf expansion. Plant Physiol **143:** 1905–1917

Vanrensburg L, Kruger GHJ (1993) Comparative analysis of differential drought stress-induced suppression of and recovery in carbon dioxide fixation: stomatal and nonstomatal limitation in *Nicotiana tabacum* L. J Plant Physiol **142:** 296–306

Veselova SV, Farkhutdinov RG, Veselov DS, Kudoyarova GR (2006) Role of cytokinins in the regulation of stomatal conductance of wheat seedlings under conditions of rapidly changing local temperature. Russ J Plant Physiol **53:** 756–761

von Caemmerer S (2000) Biochemical Models of Leaf Photosynthesis. Commonwealth Scientific and Industrial Research Organization Publishing, Victoria, Australia

von Caemmerer S, Farquhar GD (1981) Some relationships between the biochemistry of photosynthesis and the gas-exchange of leaves. Planta **153:** 376–387

Wang J, Letham DS, Cornish E, Wei K, Hocart CH, Michael M, Stevenson KR (1997) Studies of cytokinin action and metabolism using tobacco plants expressing either the ipt or the GUS gene controlled by a chalcone synthase promoter ipt and GUS gene expression, cytokinin levels and metabolism. Aust J Plant Physiol **24:** 673–683

Wingler A, Lea PJ, Quick WP, Leegood RC (2000) Photorespiration: metabolic pathways and their role in stress protection. Philos Trans R Soc Lond B Biol Sci **355:** 1517–1529

Wingler A, Quick WP, Bungard RA, Bailey KJ, Lea PJ, Leegood RC (1999) The role of photorespiration during drought stress: an analysis utilizing barley mutants with reduced activities of photorespiratory enzymes. Plant Cell Environ **22:** 361–373

Yamaguchi-Shinozaki K, Shinozaki K (2006) Transcriptional regulatory networks in cellular responses and tolerance to dehydration and cold stresses. Annu Rev Plant Biol **57:** 781–803

Yang HB, An SQ, Sung OJ, Shi ZM, She XS, Sun QY, Liu SR (2008) Seasonal variation and correlation with environmental factors of photosynthesis and water use efficiency of *Juglans regia* and *Ziziphus jujuba*. J Integr Plant Biol **50:** 210–220

Zellnig G, Peters J, Jimenez MS, Morales D, Grill D, Perktold A (2002) Three-dimensional reconstruction of the stomatal complex in Pinus canariensis needles using serial sections. Plant Biol **4:** 70–76